

III-E Spectroscopy and Dynamics of Vibrationally Excited Molecules and Clusters

This research group is studying structure and dynamics of molecules and clusters by two-color double resonance spectroscopy. New spectroscopic methods will also be developed to observe the higher vibrational state under collision-free condition.

A molecular cluster is a microscopic system of solution and/or crystal, and is thought to provide detailed information on relaxation and reaction dynamics in condensed phase. However the previous studies are concentrated to stable clusters which has no reaction pathway after photo-excitation. Consequently, spectroscopic information which concerns the reaction mechanism has not been obtained sufficiently. In this research project started from 2000, we will apply various laser spectroscopies to the reactive clusters to reveal detailed mechanism of intracuster reaction.

For the study of the ground state, the structure of the cluster can be determined by the combination of the IR dip spectroscopy and *ab initio* MO calculations.¹⁾ The IR dip spectroscopy is a kind of IR-UV double resonance spectroscopy which provides the spectrum which corresponds to the infrared absorption spectrum of the cluster (see Figure 1). A tunable IR laser is introduced to the clusters and is scanned its frequency over the fundamental vibrational region (typically 2400 ~ 4000 cm^{-1}). Then a tunable UV laser, of which the frequency is fixed to the S_1 origin of a specific cluster, is introduced and resonant enhanced multiphoton ionization signal *via* S_1 is monitored. When the IR laser is resonant to a vibrational level of the cluster, the ion signal decreases much because of loss of the population in the vibrational ground state. Thus, the IR absorption spectrum of the cluster can be measured by this depletion spectroscopy. The same spectrum can be obtained when the fluorescence intensity from S_1 is monitored instead of the ion current.

The IR spectrum in the excited state S_1 can also be measured by the depletion spectroscopy, when the UV laser is introduced before the IR laser (the UV-IR fluorescence dip spectroscopy; see Figure 2). The molecule is excited to S_1 by the UV laser, and the fluorescence intensity is monitored as well as the IR dip spectroscopy for S_0 . Then the S_1 molecules are further excited to the vibrationally excited level in S_1 by the IR laser. In general, the fluorescence quantum yield decreases in the higher vibronic level. Thus, the total fluorescence intensity decreases when the IR laser frequency is resonant to the vibrational level in S_1 .

Similarly, the IR spectrum of the ionic cluster can be measured by the depletion spectroscopy (mass-selected ion dip spectroscopy; see Figure 3). The ionic cluster can be prepared by the multiphoton ionization *via* S_1 , and the ion current due to the cation cluster of the specific size can be measured through a mass-filter. When the ionic cluster is vibrationally excited by the IR laser, the cluster is dissociated by the vibrational predissociation. Therefore, the IR transition can be measured by the decrease of the parent cluster. The same spectrum can be obtained by monitoring the enhancement of fragments (mass-selected multiphoton dissociation spectroscopy). In addition to these "dip" spectroscopies, the nonresonant ionization detected IR spectroscopy²⁾ and the PFI-ZEKE photoelectron spectroscopy³⁾ are also important tool to obtain the spectral information in the cation and the overtone states. Based on these spectroscopic techniques, we have measured the IR spectra of solvated clusters,⁴⁾ such as phenol/ammonia,⁵⁾ naphthol/alcohol,⁶⁾ carbazole/water⁷⁾ and 7-azaindole dimers,⁸⁾ and have discussed the relation among geometrical structure, electronic state and intracuster reactions.

From 2001, we have been developing the new ultrafast time-resolved IR spectroscopy for the reactive clusters. The pico second time-resolved vibrational spectroscopy is one of the ideal way to reveal the reaction mechanism directly. Here, we will demonstrate its usefulness by applying the hydrogen transfer reaction in photoexcited PhOH-

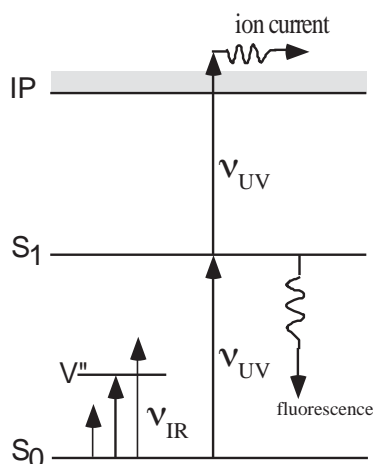


Figure 1. Principle of the IR Dip Spectroscopy. The IR transition in the ground state cluster can be measured.

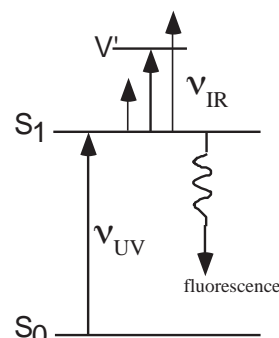


Figure 2. Principle of the UV-IR Fluorescence Dip Spectroscopy. The IR transition of the cluster in the S_1 state can be obtained.

$(\text{NH}_3)_n$ cluster.⁹⁾ Figure 4 shows the principle of the picosecond time-resolved UV-IR-UV ion dip spectroscopy. The reactive cluster ($\text{PhOH}-(\text{NH}_3)_n$ in present case) is excited to S_1 by a picosecond UV laser ν_{UV} and the photochemical reaction (hydrogen transfer) is triggered. The final reaction product, *i. e.* $(\text{NH}_3)_{n-1}\text{NH}_4$, is ionized by a nanosecond UV laser ν_{ION} which is irradiated after 100 ns from ν_{UV} and the population of the reaction product is monitored as a mass peak of $(\text{NH}_3)_{n-1}\text{NH}_4^+$. A picosecond tunable IR laser ν_{IR} is irradiated after t ps from ν_{UV} and is scanned over vibrational region. If ν_{IR} is resonant to vibrational levels of the transient species, the population of the final reaction product decreases due to the vibrational predissociation of the transient species. Therefore, the vibrational transitions of the transient species at t ps can be observed as decrease of ion current of the final reaction product.

Time resolved UV-IR-UV ion dip spectra of phenol- $(\text{NH}_3)_3$ are shown in Figure 5. The numbers in the left hand sides of each spectrum indicate the delay time from ν_{UV} to ν_{IR} . Here the spectrum at -20 ns corresponds to the IR spectrum of $\text{PhOH}-(\text{NH}_3)_3$ in S_0 , in which the sharp bands around 3400 cm^{-1} , the broad bands at $\sim 3200\text{ cm}^{-1}$ and the very broad background are assigned to the degenerated antisymmetric stretch vibration ν_3 in NH_3 , the totally symmetric stretch vibration ν_1 in NH_3 and the OH stretch vibration ν_{OH} in phenol, respectively. The spectrum at $+180$ ns shows the vibrational transitions of the final reaction product *via* S_1 , *i. e.* $(\text{NH}_3)_2\text{NH}_4$, and 1) two intense bands at 3180 cm^{-1} and 3250 cm^{-1} and 2) a broad band at $2700 \sim 3100\text{ cm}^{-1}$ which have been assigned to

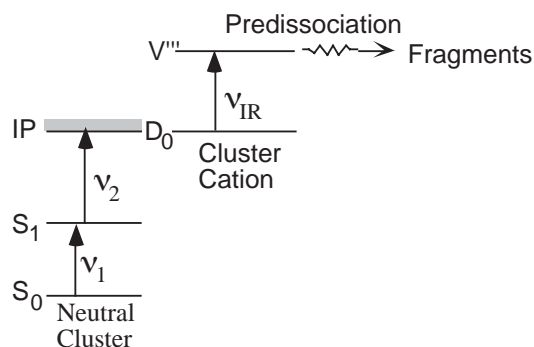


Figure 3. Principle of the mass-selected IR Ion Dip Spectroscopy. The IR transition of the cluster cation can be measured by the depletion of the parent cluster cation. The same spectrum can be measure by monitoring the enhancement of the fragments produced by the IR predissociation.

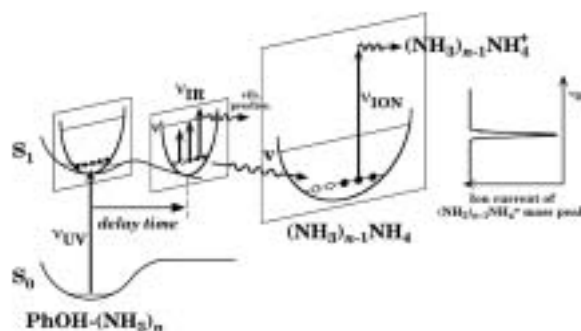
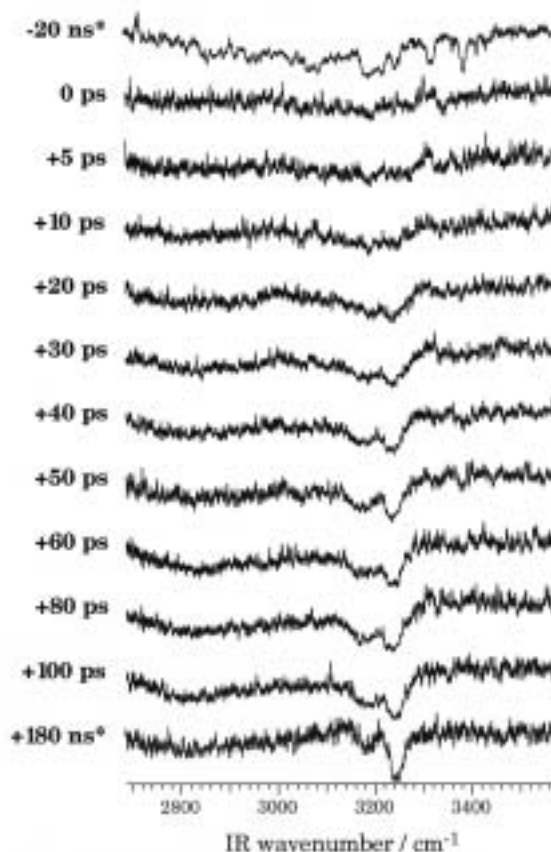


Figure 4. Principle of picosecond time-resolved UV-IR-UV ion dip spectroscopy. Potential curves of S_0 and S_1 are schematically drawn along O-H stretch coordinate. Potential curves in different sections on the S_1 O-H stretch coordinate are drawn along arbitrary N-H stretch coordinates.

Figure 5. Picosecond time-resolved UV-IR-UV ion dip spectra of the transient species from the electronically excited $\text{PhOH}-(\text{NH}_3)_3$ which was observed by fixing ν_{UV} to the low vibronic band in the S_1 state of $\text{PhOH}-(\text{NH}_3)_3$ (281.49 nm) and monitoring $(\text{NH}_3)_2\text{NH}_4^+$ due to ν_{ION} (355 nm). Times indicated at the left side of each spectrum mean the delay times between ν_{UV} and ν_{IR} . The spectra whose delay times are -20 ns and $+180\text{ ns}$ (indicated by *) are obtained by nanosecond laser system, which have been reported in the previous paper.⁵⁾



vibrational transitions concerned with NH_4 .

One can see that the vibrational bands rise with increasing delay time. The spectral feature at +100 ps is already similar to that of the final reaction product (+180 ns). Here, the intense band at 3250 cm^{-1} rises slower than the band at 3180 cm^{-1} . The relative intensities of the two bands become comparable at 40 ps, thereafter, the higher band at 3250 cm^{-1} clearly grows further. Thus, the rising time constant of the band at 3250 cm^{-1} is apparently different from that of the 3180 cm^{-1} -band. This remarkable difference between the two intense bands suggests that each vibrational transition is derived from different species. The existence of two transient species are naturally interpreted by considering the isomers of $(\text{NH}_3)_2\text{NH}_4$; the most stable $\text{NH}_3\text{-NH}_4\text{-NH}_3$ and the meta-stable $\text{NH}_4\text{-NH}_3\text{-NH}_3$. The co-existence of isomers is strongly supported by *ab initio* calculations.

As described above, we have successfully measured the picosecond time resolved IR spectra of the transient species for the ESHT of $\text{PhOH-(NH}_3)_3$ for the first time. It proves that the picosecond UV-IR-UV ion dip spectroscopy is a powerful tool to explore the dynamics of the intracuster reaction.

References

- 1) R. Yoshino *et al.*, *J. Phys. Chem. A* **102**, 6227 (1998).
- 2) T. Omi *et al.*, *Chem. Phys. Lett.* **252**, 287 (1996); S. Ishiuchi *et al.*, *Chem. Phys. Lett.* **283**, 243 (1998).
- 3) K. Takazawa *et al.*, *Chem. Phys. Lett.* **189**, 592 (1992); K. Müller-Dethlefs *et al.*, *Z. Naturforsch. Teil A* **39**, 1089 (1984); K. Müller-Dethlefs and M. C. R. Cockett, "Zero Kinetic Energy (ZEKE) Photoelectron Spectroscopy," Chapter 7, "Nonlinear Spectroscopy for Molecular Structure Determination," R. W. Field *et al.*, Eds., (Blackwell Science, Oxford, 1998), and references therein.; E. W. Schlag, "ZEKE Spectroscopy" (Cambridge University Press, Cambridge, 1998), and references therein.
- 4) K. Suzuki, Y. Emura, S. Ishiuchi and M. Fujii, *J. Electron Spectrosc.* **108**, 13 (2000), K. Suzuki, S. Ishiuchi and M. Fujii, *Faraday Discuss.* **115**, 229 (2000), K. Sakota, N. Yamamoto, K. Ohashi, H. Sekiya, M. Saeki, S. Ishiuchi, M. Sakai and M. Fujii, *Chem. Phys. Lett.* **341**, 70 (2001).
- 5) S. Ishiuchi, M. Saeki, M. Sakai and M. Fujii, *Chem. Phys. Lett.* **322**, 27 (2000).
- 6) M. Saeki, S. Ishiuchi, M. Sakai and M. Fujii, *J. Phys. Chem. A* **105**, 10045 (2001).
- 7) M. Sakai, K. Daigoku, S. Ishiuchi, M. Saeki, K. Hashimoto and M. Fujii, *J. Phys. Chem. A* **105**, 8651 (2001).
- 8) H. Yokoyama, H. Watanabe, T. Omi, S. Ishiuchi and M. Fujii, *J. Phys. Chem. A* **105**, 9366 (2001).
- 9) S. Ishiuchi, M. Sakai, K. Daigoku, T. Ueda, T. Yamanaka, K. Hashimoto and M. Fujii, *Chem. Phys. Lett.* **347**, 87 (2001).

III-E-1 Hydrogen Transfer in Photo-Excited Phenol/Ammonia Clusters by UV-IR-UV Ion Dip Spectroscopy and Ab Initio MO Calculations I: Electronic Transitions

ISHIUCHI, Shun-ichi¹; DAIGOKU, Kota²; SAEKI, Morihisa³; SAKAI, Makoto⁴; HASHIMOTO, Kenro¹; FUJII, Masaaki⁴

(¹Tokyo Inst. Tech./JST-PRESTO; ²Tokyo Metropolitan Univ./ACT-JST; ³JAERI; ⁴IMS and Tokyo Inst. Tech.)

[*J. Chem. Phys.* **117**, 7077–7082 (2002)]

The electronic spectra of reaction products *via* photo-excited phenol/ammonia clusters (1:2~5) have been measured by UV-near-IR-UV ion dip spectroscopy. Compared with the electronic spectra of hydrogenated ammonia cluster radicals the reaction products have been proven to be $(\text{NH}_3)_{n-1}\text{NH}_4$ ($n = 2 \sim 5$), which are generated by excited-state hydrogen transfer in $\text{PhOH-(NH}_3)_n$. By comparing the experimental results with *ab initio* molecular orbital calculations at multi-reference single and double excitation CI level, it has been found that the reaction products, $(\text{NH}_3)_{n-1}\text{NH}_4$ (for $n = 3$ and 4), contain some isomers.

III-E-2 Hydrogen Transfer in Photo-Excited Phenol/Ammonia Clusters by UV-IR-UV Ion Dip Spectroscopy and Ab Initio MO Calculations II: Vibrational Transitions

ISHIUCHI, Shun-ichi¹; DAIGOKU, Kota²; SAEKI, Morihisa³; SAKAI, Makoto⁴; HASHIMOTO,

Kenro¹; FUJII, Masaaki⁴

(¹Tokyo Inst. Tech./JST-PRESTO; ²Tokyo Metropolitan Univ./ACT-JST; ³JAERI; ⁴IMS and Tokyo Inst. Tech.)

[*J. Chem. Phys.* **117**, 7083–7093 (2002)]

The vibrational spectra of phenol/ammonia clusters (1:2~5) in S_0 and those of their photo chemical reaction products, $(\text{NH}_3)_{n-1}\text{NH}_4$ ($n = 2 \sim 5$), which are generated by excited-state hydrogen transfer, have been measured by UV-IR-UV ion dip spectroscopy. The geometries, IR spectra and normal modes of phenol- $(\text{NH}_3)_n$ ($n = 1 \sim 5$) have been examined by *ab initio* molecular orbital calculations, at the second-order Møller-Plesset perturbation theory level with large basis sets. For the $n = 2$ and 3 reaction products, similar vibrational analyses have been carried out. From the geometrical information of reactants and products, it has been suggested that the reaction products have memories of the reactant's structure, which we call "memory effect."

III-E-3 Picosecond Time-Resolved Nonresonant Ionization Detected IR Spectroscopy on 7-Azaindole Dimer

SAKAI, Makoto¹; ISHIUCHI, Shun-ichi²; FUJII, Masaaki¹

(¹IMS and Tokyo Inst. Tech.; ²Tokyo Inst. Tech./JST-PRESTO)

[*Eur. J. Phys. D.* **20**, 399–402 (2002)]

The picosecond time-resolved IR spectrum of the 7-

azaindole dimer has been measured by picosecond time-resolved nonresonant ionization detected IR spectroscopy. This new time-resolved technique was developed by combining nonresonant ionization detected IR (NID-IR) spectroscopy with tunable picosecond IR and UV lasers. The time-resolved NID-IR spectrum from 2600 cm^{-1} to 3800 cm^{-1} shows a drastic change from 1.5 ps to 11 ps time evolution. A mode-specific vibrational redistribution has been suggested.

III-E-4 Construction of a Picosecond Time-Resolved IR Dip Spectrometer for Studying Structures and Dynamics of Solvated Clusters

SAKAI, Makoto¹; UEDA, Tadashi; YAMANAKA, Takaya; FUJII, Masaaki¹
(¹IMS and Tokyo Inst. Tech.)

[*Bull. Chem. Soc. Jpn.* **76**, 509–514 (2003)]

We have constructed a picosecond time-resolved IR dip spectrometer having a frequency resolution of $< 20 \text{ cm}^{-1}$ and an instrument response time of 25 ps, respectively. In this system, the second harmonic of the idler wave from the OPA pumped at 800 nm and the remaining light from a regenerative amplifier ($< 2.5 \text{ mJ/pulse}$) were differentially mixed in a KTA crystal to generate tunable high-power IR light (2750–4000 cm^{-1} ; $> 60 \text{ }\mu\text{J}$). The picosecond time-resolved IR dip spectra of phenol-(H_2O)₁ and carbazole-(H_2O)₁ are presented to demonstrate the capability of the constructed system. The spectral changes show clear vibrational structures of not only S_0 , but also S_1 in the 2800–3800 cm^{-1} energy region. The system performance is also discussed.

III-E-5 Two-Color Far-Field Super-Resolution Microscope Using a Doughnut Beam

WATANABE, Takeshi¹; IKETAKI, Yoshinori²;
OMATSU, Takashige³; YAMAMOTO, Kimihisa⁴;
ISHIUCHI, Shun-ichi⁵; SAKAI, Makoto¹; FUJII,
Masaaki¹
(¹IMS and Tokyo Inst. Tech.; ²Olympus Optical Co.
Ltd.; ³Chiba Univ.; ⁴Keio Univ./JST-PRESTO)

[*Chem. Phys. Lett.* **371**, 634–639 (2003)]

We have demonstrated a realistic super-resolution scanning fluorescence microscope using conventional nanosecond lasers. This super-resolution microscope is based on the combination of two-color fluorescence dip spectroscopy and shape modulation to a doughnut beam. Only by introducing a doughnut erase beam, the resolution of the laser fluorescence microscope breaks the diffraction limit by two times without using any mechanical probe.

III-E-6 Investigation of the Fluorescence Depletion Process in Condensed Phase

IKETAKI, Yoshinori¹; WATANABE, Takeshi²;
ISHIUCHI, Shun-ichi³; SAKAI, Makoto²;
OMATSU, Takashige⁴; YAMAMOTO, Kimihisa⁵;
FUJII, Masaaki²; WATANABE, Tsutomu⁶

(¹Olympus Optical Co. Ltd.; ²IMS and Tokyo Inst. Tech.; ³Tokyo Inst. Tech./JST-PRESTO; ⁴Chiba Univ.; ⁵Keio Univ.; ⁶Univ. Electro-Communications)

[*Chem. Phys. Lett.* **372**, 773–778 (2003)]

By using a two-color dip spectroscopy, we measured the fluorescence intensity from tryptophan in a water solution. The fluorescence intensity exponentially decreased as the laser intensity for the $S_n \leftarrow S_1$ excitation increased. The phenomenon was analyzed by a rate-equation for a three-state model. The analysis shows that tryptophan with the S_n state has a radiationless relaxation process without any process through the S_1 state, and that the $S_n \rightarrow S_1$ internal conversion does not have a 100% yield. The branching ratio of the process is estimated to be 20%. The presented result clarifies in detail the real meaning of Kasha's rule.